Near-Infrared Acousto-optic Filtered Spectroscopic Microscopy: A Solid-State Approach to Chemical Imaging

PATRICK J. TREADO, IRA W. LEVIN, and E. NEIL LEWIS*

Laboratory of Chemical Physics, National Institute of Diabetes and Digestive and Kidney Diseases, National Institutes of Health, Bethesda, Maryland 20892

A new instrumental approach for performing spectroscopic imaging microscopy is described. The instrument integrates an acousto-optic tunable filter (AOTF) and charge-coupled-device (CCD) detector with an infinity-corrected microscope for operation in the visible and near-infrared (NIR) spectral regions. Images at moderate spectral resolution (2 nm) and high spatial resolution (1 μm) can be collected rapidly. Data are presented containing 128 × 128 pixels, although images with significantly larger formats can be collected in approximately the same time. In operation, the CCD is used as a true imaging detector, while wavelength selectivity is provided by using the AOTF and quartz tungsten halogen lamp to create a tunable source. The instrument is entirely solid state, containing no moving parts, and can be readily configured for both absorption and reflectance spectroscopies. We present visible absorption spectral images of human epithelial cells, as well as NIR vibrational absorption images of a hydrated phospholipid suspension, to demonstrate the potential of the technique in the study of biological materials. Extensions and future applications of this work are discussed.

Index Headings: **Instrumentation, imaging; Spectroscopic techniques; Near-infrared spectroscopy; Visible spectroscopy; Acousto-optics; Charge-coupled devices; Histology; Phospholipids.**

INTRODUCTION

Spectroscopic imaging, the determination of spatially distributed and chemically distinct species in heterogenous materials, is a powerful analytical tool that has been applied to both macroscopic and microscopic imaging. Chemical imaging of large areas (>20 km²) is routinely performed with airborne and spaceborne remote-sensing imaging spectrometers.[1] On a smaller scale, nuclear magnetic resonance techniques[2] are applied for whole-body diagnostic imaging. For investigation of the microscale, fluorescence microscopy[3,4] is an effective chemical state imaging tool, particularly when employing highly specific immunofluorescent tags. Vibrational spectroscopic imaging techniques, Raman[5] and infrared[6] microscopy, provide widely applicable chemical selectivity without sample preparation.

Received 23 November 1991.

* Author to whom correspondence should be sent. Address for correspondence: National Institutes of Health, Building 2, Room 114, Bethesda, Maryland 20892.

While the spectroscopic experimental requirements vary widely, two primary methods are employed for image generation. One method involves scanning of the sample systematically through a stationary field of view defined by the collection optics and detector. Alternatively, the imaging source (or detector) can be scanned in a raster pattern across the surface of the stationary sample. The scanning approach is utilized most often with single-element detection. Fourier transform infrared (FT-IR) functional group imaging utilizing a mid-infrared microscope outfitted with an xy mapping translation stage[7,8] is one tool that employs the scanning method. The signal-to-noise ratio obtainable with this technique often requires signal averaging at each spatial position, making FT-IR microscopy an inherently slow technique. As a result, only crude spatial maps are often practical. Where signal is abundant—in laser scanning fluorescence microscopy, for example—high visual clarity images can be acquired in real time.

Another image generation approach involves wide field illumination and viewing and is used where multichannel detection is feasible. The simplest implementation involves sample illumination with a broad-band visible source and direct viewing with a color video camera. The colorometric information is due to visible absorption of the sample. This approach is widely used in video microscopy of biologics and materials.[9] Where greater specificity and selectivity are required, optical filtering can be employed. For example, fluorescence microscopes filter the light source to selectively excite within the absorption band of the fluorescent label. Long-pass emission filters are used to attenuate nonfluorescent reflected excitation energy as well as stray light prior to imaging with a sensitive camera. Multiple fluorescent labels can be used with dielectric filters, which provide several bandpass regions for detecting numerous spectral bands simultaneously.[10] The bandpass filter approach is adequate where relatively low spectral resolution (>5 nm) is sufficient and broad tunability is unnecessary. Where both spectral tunability and rapid operation are desired, an acousto-optic-based system that has been developed for fluorescence spectroscopy[11] may also be applicable to

0003-7028/92/4604-0553$2.00/0

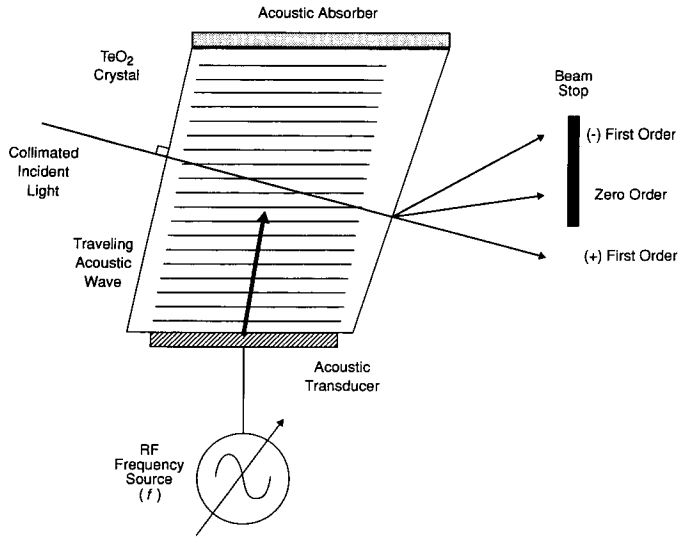

FIG. 1. Schematic representation of an AOTF crystal showing an rf frequency source and a traveling acoustic wave. The crystal facets are cut in such a manner that the selected first-order beam exits the crystal approximately colinearly with the incident white light source, significantly easing alignment of the optical train.

fluorescence imaging. In Raman and mid-infrared imaging, moderate spectral resolution (<1 nm) and broad tunability are obtained through a hybrid multichannel/multiplex approach employing Hadamard transform spatial multiplexing.[12]

In this communication we describe an entirely solid-state, no-moving-parts approach to spectroscopic imaging. This novel technique integrates an acousto-optic filtered broad-band light source with an optical microscope and a high-dynamic-range, charge-coupled-device (CCD) detector for rapidly generating spectroscopic images. With this system of moderate spectral resolution, spectral images of sub-micron spatial resolution having 128 × 128 pixels are readily collected.

THEORY

Acousto-optic Filter. The principles and theory of operation of acousto-optic (A-O) deflection and modulation devices have long been established,[13–15] although their use as spectroscopic filters or monochromators has been limited. Briefly, an acousto-optic tunable filter (AOTF) can be considered as an electronically tunable spectral bandpass filter which can operate from the UV through the visible and into the infrared regions of the optical spectrum. The filters function by the interaction of light with a traveling acoustic wave through an anisotropic medium. As shown in Fig. 1, an acoustic transducer is bonded to one end of a crystal, while an acoustic absorber is bonded to the other. The transducer converts a high-frequency rf signal of frequency f_a into a pressure wave which propagates laterally through the crystal with a velocity v_a. The acoustic absorber at the opposite end of the crystal serves to eliminate acoustic reflections which corrupt the primary acoustic waveform. The diffracted wavelengths are self-selected within the A-O crystal to satisfy the momentum conservation between the incident $\mathbf{k}_i$ and diffracted $\mathbf{k}_d$ photon wave vectors and the acoustic wave vector $\mathbf{k}_a$ as described by

$$\mathbf{k}_d = \mathbf{k}_i \pm \mathbf{k}_a. \quad (1)$$

Optical tuning, achieved by changing the rf frequency f_a, is given by

$$\lambda_o = v_a(n_e - n_o)a/f_a \quad (2)$$

where n_e and n_o are the refractive indices of the extraordinary and ordinary wave, respectively, and a is a parameter depending upon the design of the AOTF. The acoustic wave may be considered the means for generating a transmission grating within the optical crystal. Instead of varying the angle of the incident beam, as would be the case for a normal diffraction grating in order to achieve wavelength selectivity, one varies the frequency of the electrical drive signal, allowing light of different wavelengths to be diffracted at the same angle. Hence, with a fixed orientation of the crystal and the use of an rf generator, a tunable optical source is readily created from a broad-band source. An additional and very powerful feature of the AOTF stems from the ability to control the intensity of the diffracted beam by varying the amplitude or the amount of rf power applied to the crystal. This approach can also be used to rapidly modulate, or chop, the filtered source for lock-in detection schemes.

The AOTF crystal used in the present experiments was constructed from tellurium dioxide (TeO_2); the rf frequencies varied from 40 to 170 MHz, for wavelength operation between 400 and 1900 nm. The device has a resolution of approximately 2.5 nm and an achievable tunability of approximately 0.1 nm with a wavelength repeatability of better than 0.05 nm. TeO_2 may be used to design AOTF devices from approximately 500 to 5500 nm. For any given crystal, the resolution is fixed but may be varied by changing the acousto-optic interaction distance at the time of manufacture. The devices are entirely solid state, containing no moving parts, and may be considered to be random-access filters where tuning from one wavelength to another is achieved in the time it takes for the acoustic wave to propagate the full length of the crystal, typically 5 μs.

AOTF Principles in Imaging Spectroscopy. The AOTF imaging spectrometer may be used in one of two ways. The more straightforward approach is specific to absorption spectroscopy and is the method employed in this work, while the second method may be applied to both absorption and emission spectroscopies.

In the first approach, the filter is used as a narrow bandpass filter and is placed directly in front of a broad-band source. In this way only light of the selected wavelength is transmitted for subsequent interaction with the sample before being imaged by a focal plane array detector. In the second scheme, a broad-band source may be allowed to impinge on the sample, while the AOTF is placed in front of the imaging detector. This second method has been discussed with reference to fluorescence imaging,[11] but is also suited to Raman imaging techniques. An advantage of source filtering, particularly for absorption spectroscopic studies of biological materials, is the greatly reduced optical power densities incident on a sample. These reduced power densities have the effect of minimizing both the thermal and photochemical degradation of the sample.[16]

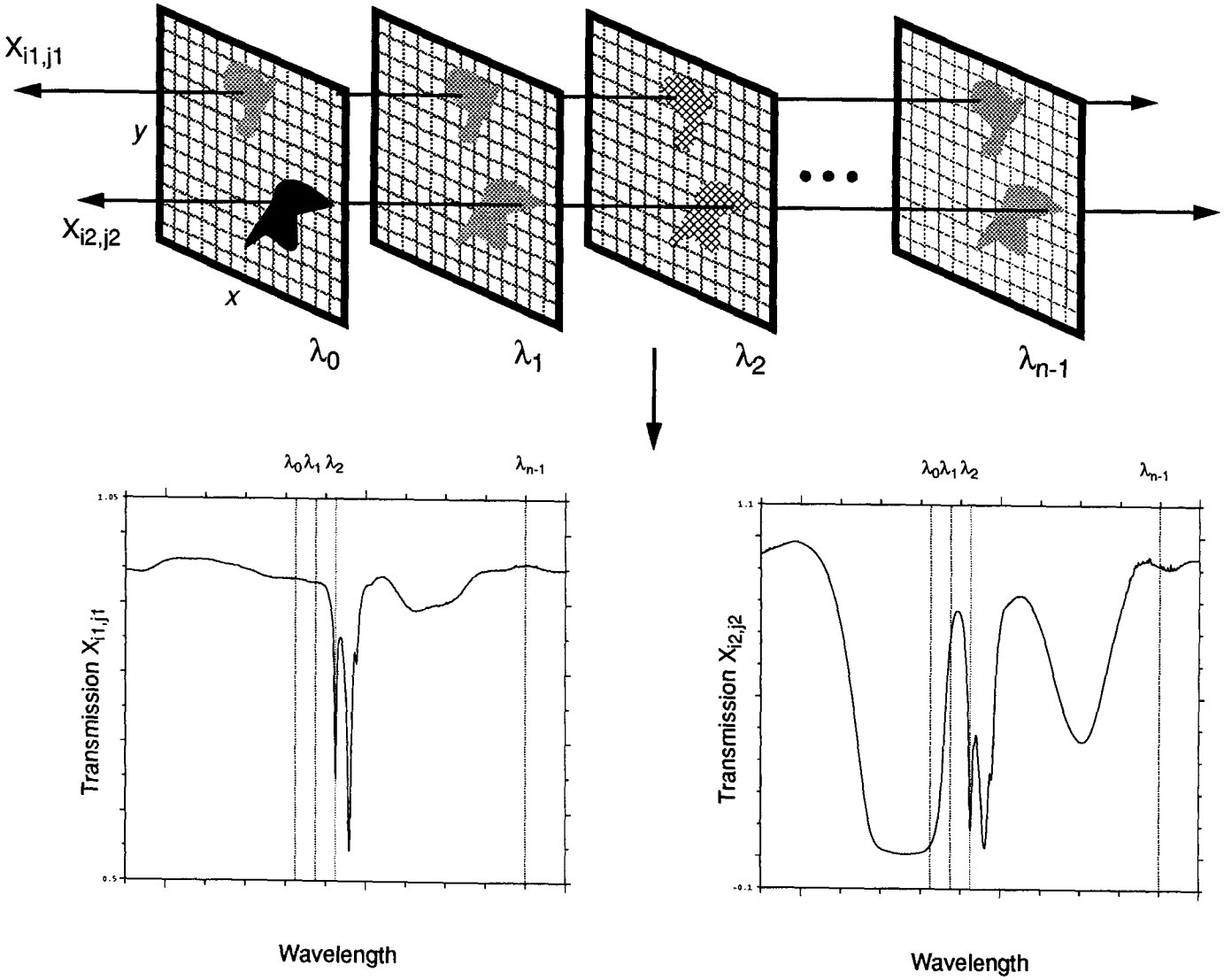

FIG. 2. A pictorial view of the typical data set acquired by the imaging spectrometer. In the upper panels, the data are presented as a series of stacked images at sequential and discrete wavelengths, which represents the format in which data are actually collected. In the lower panels a series of transmission values are extracted from different images at two fixed but different image coordinates, therefore depicting the absorption spectra of two spatially and chemically distinct regions of the sample.

When used as a tunable source, the A-O filter method of data acquisition is straightforward. The filter sweeps through hundreds of nanometers at predetermined wavelength intervals, recording one frame with the focal plane array detector at each wavelength interval. Hundreds or even thousands of frames may be collected, where a full data set may readily comprise many megabytes of data. As modeled in Fig. 2, the data are considered either as separate sample images at different wavelengths or as a series of individual absorption spectra for each pixel element in the image. Alternatively, the AOTF may be tuned to various wavelengths corresponding to known absorption maxima, while numerous spectral frames can be collected at each specified wavelength. These frames may be collected rapidly over a period of several seconds or far more slowly over time frames extending to hours or days. Images may be constructed that yield information on both the spatial and temporal properties of a sample with respect to highly selective spectroscopic markers.

EXPERIMENTAL PROCEDURES

Figure 3 is a schematic of the A-O filtered spectroscopic microscope. The system integrates a visible/near-infrared tellurium dioxide (TeO_2) AOTF (Brimrose TEAF-.6-.1.2L) with a research-grade, infinity-corrected, metallurgical microscope (Olympus BH-2). The microscope employed 10× (N.A. 0.30) and 20× (N.A. 0.46) plan achromat objectives and a 2.5× projection eyepiece for image collection, magnification, and presentation to the detector. Image detection is provided by a low-noise, high-dynamic-range (16 bits) CCD (Spex Spectrum One) having 576 × 384 pixels, each 20 μm square. The detector is cooled to cryogenic temperatures (−140°C) with liquid N_2.

In operation, the AOTF is used to spectrally filter a collimated and stabilized 50-W quartz tungsten halogen light source (Newport 780). Collection and collimation is performed with an $f/1$ quartz lens. Under computer control, individual wavelengths are selected with digital

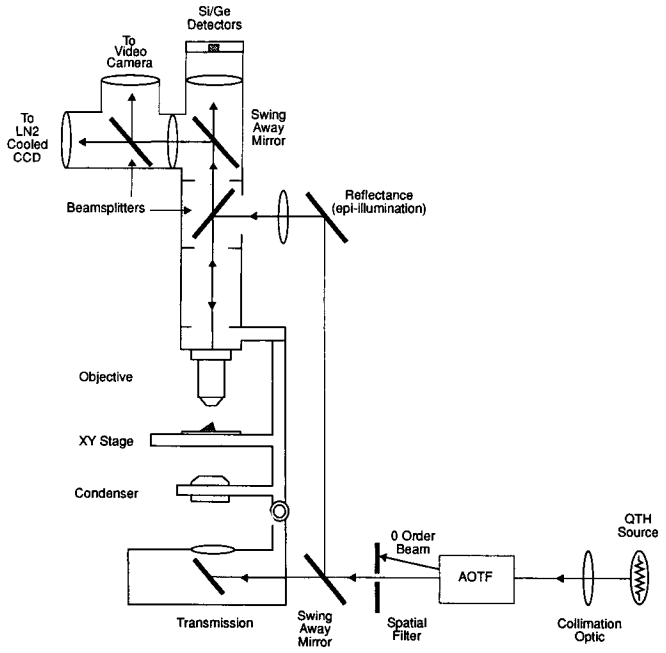

FIG. 3. Schematic diagram of the imaging spectrometer optical train. The figure shows the arrangement of the modified microscope with respect to the AOTF illumination scheme for both transmission and reflectance measurements, as well as the relative positions of the CCD, video camera, and point detector.

precision to yield approximately monochromatic light from the broad-band visible/near-infrared source. The (+) diffracted order of the AOTF is selected with an aperture which simultaneously blocks the fundamental beam as well as the (−) diffracted order light. The (+) and (−) diffracted orders differ only in polarization and deflection angle. Theoretically the (−) order could be combined with the (+) order beam for a 2× increase in illumination intensity. The apertured beam is directed by a swing-away mirror to either the transmission port or the epi-illumination reflectance port of the microscope. The choice of transmission or reflectance operation depends on the sample opacity. In transmission, an Abbe condenser provides Koehler illumination.

Prior to imaging of the sample, microspectroscopy must often be performed for unknown materials to provide survey spectral characterization. Microspectroscopy is performed by selectively illuminating the region of interest with the tuned light source through a small aperture, and detection is performed with a single-element photodiode. In this manner the instrument acts as a microprobe. While the A-O spectroscopic microscope does provide point spectra, operation of the slow-scan CCD is time consuming, on the order of minutes for spectra covering the full wavelength range at high resolution. In contrast, the AOTF is capable of very fast operation, requiring only milliseconds to sweep the same range. By incorporating fast, single-point detection into the system design, we can acquire survey spectra very rapidly. For visible wavelength operation (400–1100 nm) a silicon photodiode is used, while near-infrared sensitivity (800–1800 nm) is provided by a germanium detector sampled with a 12-bit A/D converter (National Instruments AT-MIO-16L). Signal levels decrease as the field of view is apertured down, and the detectors are operated uncooled, requiring signal averaging for improved signal-to-noise performance. Typically, several hundred averages are performed, which increases the acquisition time to several seconds.

Upon spectral characterization, imaging can be performed. A swing-away mirror directs light away from the single-point detector and towards the imaging camera. A lens positioned after the swing-away mirror forms an intermediate image of the collected light, which is magnified by the infinity-corrected objective. The intermediate image is split by a 50/50 cube beamsplitter directing light to identical 2.5× projection eyepieces. The eyepieces provide additional magnification and present flat-field spectral images to the low-light-level CCD and a video CCD camera (Javelin), simultaneously. The video camera is parfocal with the low-light-level CCD and is used with a video monitor (Ikegami) for sample positioning and focusing. Samples are viewed on glass microscope slides.

An 80386-based computer (Del 310) was used for spectral image collection and processing. Software was written primarily in the C programming language to integrate data acquisition and control in a coherent fashion. Primary spectral image processing was also performed with the use of computer software especially written to store and manipulate the data as 32-bit floating point numbers instead of the 8 bits usually handled by image processing packages. This additional precision is necessary to be able to measure the weak vibrational absorptions, which are superimposed on the instrument response function and background contributions. Contrast enhancement, pseudo-coloring, and image presentation were performed with the use of a commercial image-processing package (BioScan Optimas 3.0) and a VGA graphics board (Univision Scorpion 16G). For publication, images were photographed from the computer monitor.

A thin section of human epithelia stained with hematoxylin-eosin according to standard histological procedures[17] was used as a sample for visible absorption imaging. NIR absorption microscopy was performed on suspensions of dioleoylphosphatidylethanolamine (DOPE) (Avanti Polar Lipids) in water. Prior to imaging, the DOPE suspension, a model lipid membrane assembly, was cycled through its phase transition several times and then sonicated for 10 min to promote single-shell vesicle formation.

RESULTS

In establishing the feasibility of this approach to spectroscopic imaging, we have recorded data of many different kinds of materials in both transmission and reflection modes from 400 to 1200 nm. For the purpose of this discussion, we have selected data sets which emphasize its applicability to biological materials in both the visible and near-infrared portions of the spectrum.

Figure 4 presents spectral data and images recorded with the A-O filtered spectroscopic microscope of a cross section of human epithelia. Total magnification provided a spatial resolving element of approximately 2.0 μm per pixel. The reference bar in Fig. 4C corresponds to 14 μm. Images were recorded over the wavelength range 400 to

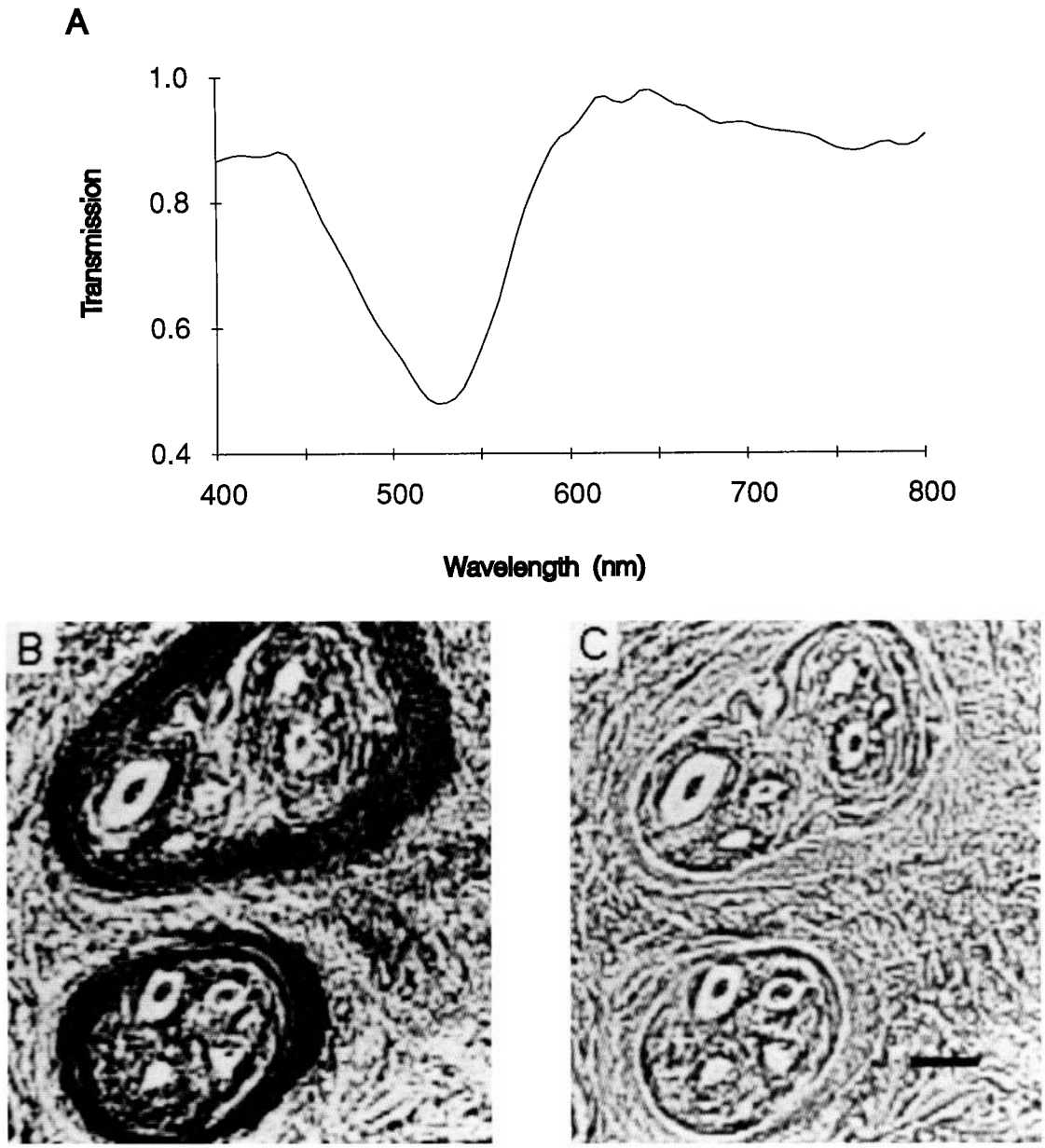

FIG. 4. A-O spectroscopic images of a cross section of human epithelial cells, stained with a visible dye, taken at 520 nm (**B**) and 710 nm (**C**), respectively. Panel **A** displays a transmission vector extracted from this data set at an x, y coordinate corresponding to one of the dark regions in image **B**. The resulting visible absorption spectrum is that of the hematoxylin-eosin stain. The reference bar in panel **C** corresponds to 14 μm.

800 nm at 2-nm increments with the use of a 15-ms exposure at each wavelength, giving a total measurement time of 3 s. With system overhead the total acquisition time was approximately 3 min. The visible absorption spectrum shown in Fig. 4A was produced by extracting 201 absorption values from a particular image x, y coordinate. The spectrum corresponds to a pixel coordinate from within the arterial wall which appears as a dark area in the image in Fig. 4B.

The images in Fig. 4B and 4C correspond to CCD exposures taken at 520 and 710 nm, respectively, It is clear that significantly higher visual clarity and structural information are available from image 4B, corresponding to the image based upon the absorption maximum of the histological stain at 520 nm. In image 4C, outside the spectral characteristics of the staining material, the outline of the arterial wall is barely visible. The apparent contrast in image 4B is a clear demonstration of chemical differences in the arterial wall relative to the bulk material in this particular tissue type.

Displaying near-infrared vibrational absorption spectra obtained with the AOTF, Fig. 5A and 5B show the transmission spectra of water in 1.0-cm- and 0.1-cm-pathlength quartz cells, respectively. The AOTF operates here as a miniature spectrometer by filtering the quartz tungsten halogen lamp source. A germanium photodiode is used for detection. In operation, the samples are placed in the nearly monochromatic beam between the AOTF and the photodiode. The resulting spectra were ratioed against a reference to obtain the transmission spectra shown. Spectra in Fig. 5A and 5B consist of 500 averages each and were obtained in approximately

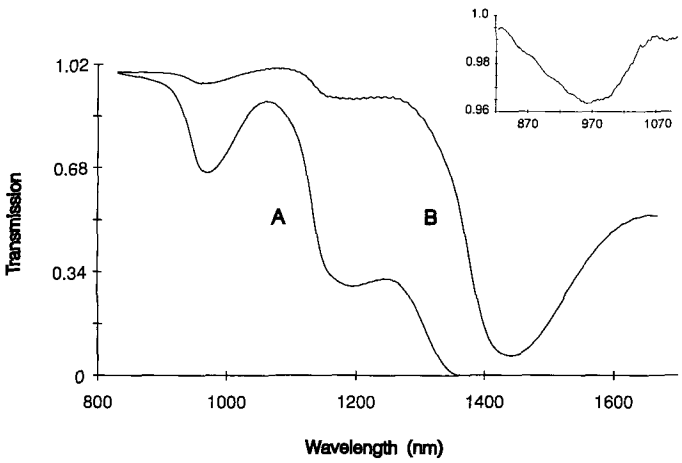

FIG. 5. Near-infrared vibrational absorption spectra of water collected between 800 and 1700 nm with an AOTF for 1.0 cm (*A*) and 0.1 cm (*B*) pathlengths, respectively, with the use of germanium photodiode. Spectra represent 500 averages collected in 3 s each. The insert displays a water spectrum corresponding to a single pixel extracted from a series of water droplet images collected under the microscope between 820 and 1100 nm with the A-O imaging spectrometer using CCD detection. The second overtone of the OH stretching mode at 960 nm is weak but clearly visible.

3 s. Notable features include the second overtone of the OH stretching mode at 960 nm, an H_2O combination band at 1190 nm, and the first overtone of the OH stretching mode at 1440 nm. In addition, a transmission spectrum of the second overtone region of water obtained with the AOTF coupled through the microscope and with the use of the silicon CCD for detection is shown in the inset. The sample for this spectrum is a pure water droplet, approximately 100 μm in diameter, deposited on the microscope slide. Assuming that the water droplet takes a spherical shape, the maximum pathlength is approximately 100 μm. The spectrum is extracted from spectral images collected between 820 and 1100 nm at 5-nm intervals and corresponds to a pixel in the center of the water droplet. An integration time of 3 s per frame was required to obtain this spectrum due to the extremely low quantum efficiency of the silicon detector (<5%) beyond 900 nm.

The spectra of Fig. 5 demonstrate the effect of sample pathlength on the vibrational absorption signal intensity shown here in transmission mode. Given the limited pathlength of microscopic materials (<100 μm), only strong vibrational absorbers are readily accessible with a silicon detector. In fact, the band at 960 nm is the only vibrational absorption accessible to our CCD without the use of exhaustive signal averaging. By extending the operation of our instrument to longer wavelengths with an appropriate detector, one could access the first overtone of the OH stretch at 1440 nm, which would then provide an increase of over two orders of magnitude in signal intensity. This is demonstrated in Fig. 5B for the single-point detection case. In general, the use of near-infrared detectors and significantly longer vibrational wavelengths would provide greater chemical selectivity and sensitivity, resulting in significantly higher image contrast.

Figure 6 shows A-O filtered spectral images of dioleoylphosphatidylethanolamine (DOPE) vesicle dispersions in water. The 128 × 128 pixel images were obtained with a 20× (N.A. 0.50) objective, which provides spatial resolution of 1.0 μm per pixel. Absorption images were recorded by tuning the AOTF to wavelengths characteristic of the OH stretching mode second overtone at 960 nm. In addition, background spectral images were obtained at wavelengths off the water absorption band for reference and comparison. We acquired images at 850, 900, and 960 nm, using exposures of 0.25, 2, and 6 s, respectively. Different integration periods are used to accommodate for the varying quantum efficiency of the CCD detector.

As seen in Fig. 4B and 4C, strongly absorbing materials provide sufficient image contrast without additional enhancement when viewed in transmission. For very weakly absorbing materials, like the DOPE lipid suspensions used in Fig. 6, pure transmission does not provide adequate contrast to differentiate between the absorbing 960-nm image (Fig. 6A) and the nonabsorbing 850-nm image (Fig. 6B). Vibrational absorption, however, is not the only contribution to sample opacity. Therefore, contributions to the sample optical density, which include refraction, reflection, scattering, etc., must be eliminated, or at least reduced sufficiently, in order to be able to unequivocally attribute sample contrast to a vibrational absorption. We accomplish this by first ratioing an image taken within the absorption band against some reference collected at the same wavelength and under identical conditions, but without sample present. This ratio removes wavelength-dependent contributions due to instrument response. The resulting image is ratioed a second time against an image collected off the absorption band to remove contributions to sample opacity (and therefore contrast) not due to sample absorption.

Figure 6A represents the OH stretching mode overtone absorption image of water obtained by ratioing the 960-nm spectral image to the 900-nm frame. Figure 6B is a nonabsorbing image obtained by ratioing the 850-nm frame to the 900-nm frame. Image contrast is superior in Fig. 6A due to absorbance of the water encapsulated within the DOPE single-shell vesicles. This particular image is especially striking since it represents the ability to achieve chemically selective image contrast in biological materials without resorting to staining. That is, the technique relies on the sample's intrinsic absorptivity as a result of its vibrational modes. The light and dark concentric rings that appear around the vesicle suspensions in Fig. 6 are classic two-dimensional diffraction patterns. The optical interference effects are accentuated by the nearly coherent light employed for sample illumination.

FUTURE DIRECTIONS

This paper has presented images derived from the visible and near-infrared absorption data collected from two distinct biological samples. While these are preliminary data, an obvious and important extension of this technique is to collect spectra at much longer wavelengths where absorption bands may be several orders of magnitude more intense. Although the present study obtained near-infrared absorption data with the use of a silicon CCD detector with sensitivity not extending much

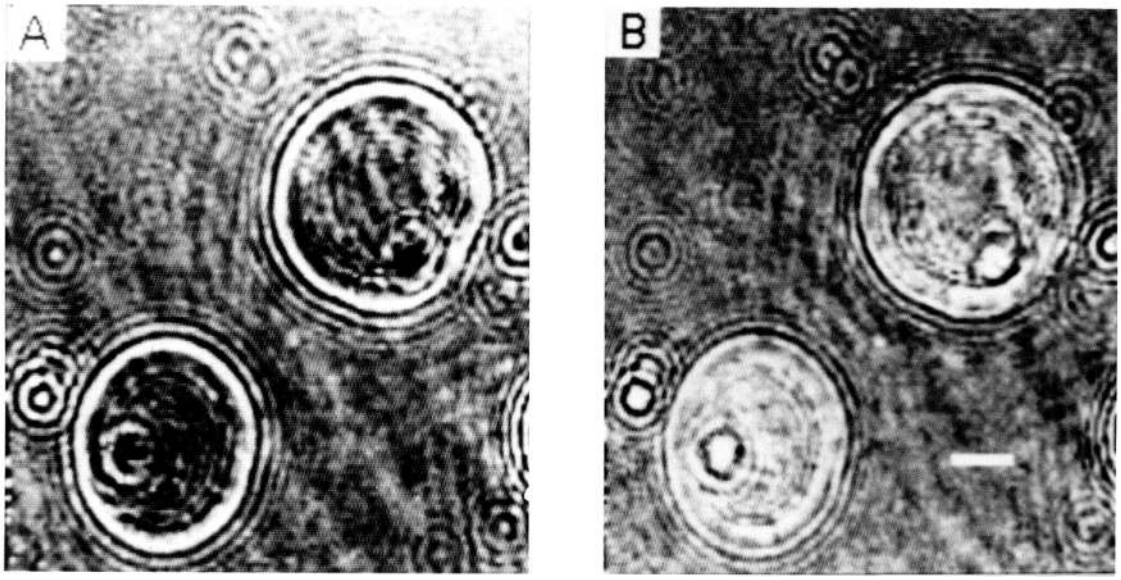

FIG. 6. Images of lipid vesicle suspensions in water collected at 960 nm (**A**) and 850 nm (**B**). The darkening of the droplets in panel **A** relative to panel **B** corresponds to the vibrational absorption of water at 960 nm. For presentation, the images are corrected for instrument response and background contributions. The reference bar in panel **B** corresponds to 5 μm.

beyond 1050 nm, recent advances in infrared focal plane array detectors will enable extension of this spectral imaging technique to 5500 nm using InSb and PtSi, to 8000 nm using IrSi, and to 12,000 nm using MCT. TeO_2 acousto-optic tunable filters are usable to approximately 5500 nm, while other materials are available for longer wavelengths. The use of these filter/detector combinations, in conjunction with an all-reflecting, achromatic infrared microscope, promises to yield a potent analytical and biomedical tool.

By placement of the solid-state optical filter directly in front of the focal plane array, both fluorescence and Raman imaging experiments may be undertaken. For the latter, however, even though crystals providing higher spectral resolution than our present one are available, the relatively large spectral bandpass characteristic of the AOTF will offer serious limitations. However, since other filter technologies, such as tunable Fabry-Perot etalons, claim 0.1 nm or better in resolution, over narrower wavelength ranges, they may be better suited to specific applications.

Since this technique provides a convenient spectroscopic imaging tool, the potential areas of application strongly overlap those techniques where traditional absorption or emission spectroscopic approaches have proven valuable. These areas could include, but not necessarily be limited to, biological materials, polymers, semiconductors, and even remote sensing. The ability to rapidly and simultaneously record thousands of absorption spectra, with little or no time penalty for collecting images at high spatial resolution, yields an exceptionally powerful technique in which various projections of the collected data sets can be manipulated to reveal subtle molecular arrangements not determinable by other spectroscopic techniques. Additionally, integration of conventional image enhancement techniques with chemometric methods reserved for the analysis of more traditional spectroscopic data provides flexibility in processing the complex data sets recorded by A-O spectroscopic microscopy.

ACKNOWLEDGMENTS

We wish to thank Dr. Jolanta Soos of The Brimrose Corp. for useful discussions regarding AOTF design and theory.

1. A. F. H. Goetz, G. Vane, J. E. Solomon, and B. N. Rock, Science **228,** 1147 (1985).
2. J. A. Kalmar, J. J. Eick, C. R. Merritt, S. E. Schuler, K. D. Miller, G. B. McFarland, and J. J. Jones, Orthopedics **11,** 417 (1988).
3. *Methods in Cell Biology,* D. L. Taylor and Y. L. Wang, Eds. (Academic Press, New York, 1989), Vol. 30.
4. K. L. Kirk, Comments Mol. Cell Biophys. **5,** 351 (1989).
5. P. J. Treado and M. D. Morris, Spectrochim. Acta Rev. **13,** 355 (1990).
6. P. J. Treado and M. D. Morris, in *Spectroscopic and Microscopic Imaging of the Chemical State,* M. D. Morris, Ed. (Marcel Dekker, New York, 1992), submitted for publication.
7. M. A. Harthcock and S. C. Atkin, Appl. Spectrosc. **42,** 449 (1988).
8. D. R. Kodali, D. M. Small, J. P. Powell, and K. Krishnan, Appl. Spectrosc. **45,** 1310 (1991).
9. S. Inoue, *Video Microscopy* (Plenum Press, New York, 1986).
10. Photonics Spectra **25,** 126 (1991).
11. I. Kurtz, R. Dwelle, and P. Katzka, Rev. Sci. Instrum. **58,** 1996 (1987).
12. P. J. Treado and M. D. Morris, Appl. Spectrosc. **44,** 1 (1990).
13. S. E. Harris and R. W. Wallace, J. Opt. Soc. Am. **59,** 744 (1969).
14. J. A. Kusters, D. A. Wilson, and D. L. Hammond, J. Opt. Soc. Am. **64,** 434 (1974).
15. I. C. Chang, Appl. Phys. Lett. **25,** 370 (1974).
16. E. N. Lewis, V. F. Kalasinsky, and I. W. Levin, Anal. Chem. **60,** 2658 (1988).
17. K. E. Johnson, *Histology and Cell Biology* (Harwal, Media, Pennsylvania, 1991).